ISSN 1070-3632, Russian Journal of General Chemistry, 2015, Vol. 85, No. 7, pp. 1725–1733. © Pleiades Publishing, Ltd., 2015.

Synthesis, Spectral, DFT, and Semi-Empirical Study of Trimetallic Complexes with Pyrazole-3,5-dicarboxylic Acid Containing Sn(IV) and Hg(II)[1]

A. Abbas[a], S. Ali[b], S. Shahzadi[b], S. K. Sharma[c], and K. Qanungo[c]

[a] *Department of Chemistry, GC University, Faisalabad, Pakistan*

[b] *Department of Chemistry, Quaid-i-Azam University, Islamabad-45320, Pakistan*
e-mail: drsa54@yahoo.com; sairashahzadi@hotmail.com

[c] *Deptartment of Science and Humanities, Faculty of Engineering and Technology,*
Mody University of Science and Technology, Lakshmangarh-332311, District Sikar, Rajasthan, India

Received April 3, 2015

Abstract—Trimetallic compounds have been synthesized by treating pyrazole-3,5-dicarboxylic acid with CS_2, di-, and triorganotin(IV) chlorides and $HgCl_2$ under reflux. The complexes have been characterized by elemental analysis, IR, ^1H and ^{13}C NMR spectroscopy. Dipole moments and charges were calculated by the semi-empirical method. Two complexes were studied by DFT (BLYP/3-21G, B3LYP-3-21G) and semi-empirical methods (PM3, PM6, MNDO, AM1, *ab initio*). IR data indicated that Sn was attached to oxygen of the carboxylic groups in a bidentate manner and adopted trigonal bipyramidal geometry. Hg was bonded to both S atoms of a ligand and exhibited square planner geometry in solid state. NMR data confirmed the four coordinated geometry of compounds in solutions.

Keywords: pyrazole-3,5-dicarboxylic acid, Sn(IV), Hg(II), spectroscopic studies, semi-empirical study, DFT, dipole moments, charge calculations, EPS map

DOI: 10.1134/S1070363215070269

INTRODUCTION

Organotin(IV) complexes have been the subject of interest due to their biomedical and commercial applications [1]. Several organotin(IV) complexes were efficient as antimicrobial [2] and antiviral agents. Applications of metal complexes in treatment of numerous human diseases have been developed [3, 4]. Biochemical activity of organotin(IV) carboxylates is greatly influenced by the structure of corresponding molecules and the coordination number of tin atoms [5–8].

Having in view the above applications and our prior study of synthesis and characterization of heterobimetallic complexes [9], we synthesized trimetallic complexes of pyrazole-3,5-dicarboxylic acid containing Sn(IV) and Hg(II). The complexes were characterized by elemental analysis, FT-IR, ^1H and ^{13}C NMR spectroscopy. Dipole moments, charges and EPS map were calculated by DFT and some semi-empirical methods.

EXPERIMENTAL

The organic solvents, pyrazole-3,5-dicarboxylic acid and $HgCl_2$ were purchased from Merck (Germany). Carbon disulfide, acetone and ethanol were purchased from Riedel-de Haen (Germany). Organotin(IV) halides were purchased from Aldrich (USA). All solvents were purified and dried by the reported methods [10]. Melting points were measured on an electrothermal melting point apparatus; model Stuart SMP3 in capillary tubes. Elemental analysis was carried out on a CHNS-932 Leco (USA) apparatus. FT-IR spectra were recorded as KBr/CsBr discs by Perkin Elmer 1000 spectrophotometer in the frequency range of 4000–250 cm^{-1}. ^1H and ^{13}C NMR spectra were recorded on a Bruker AM-300 MHz FT-NMR spectrometer using $CDCl_3$ as an internal reference.

The semi-empirical calculations were done by MOPAC 2007 [11] program in gas phase using the

[1] The text was submitted by the authors in English.

Scheme 1.

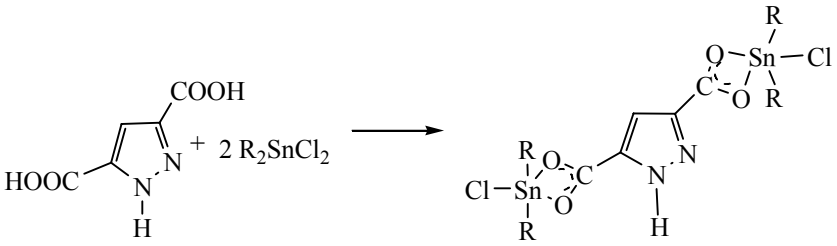

R = Me (**I**), *n*-Bu (**II**), Ph (**III**).

Scheme 2.

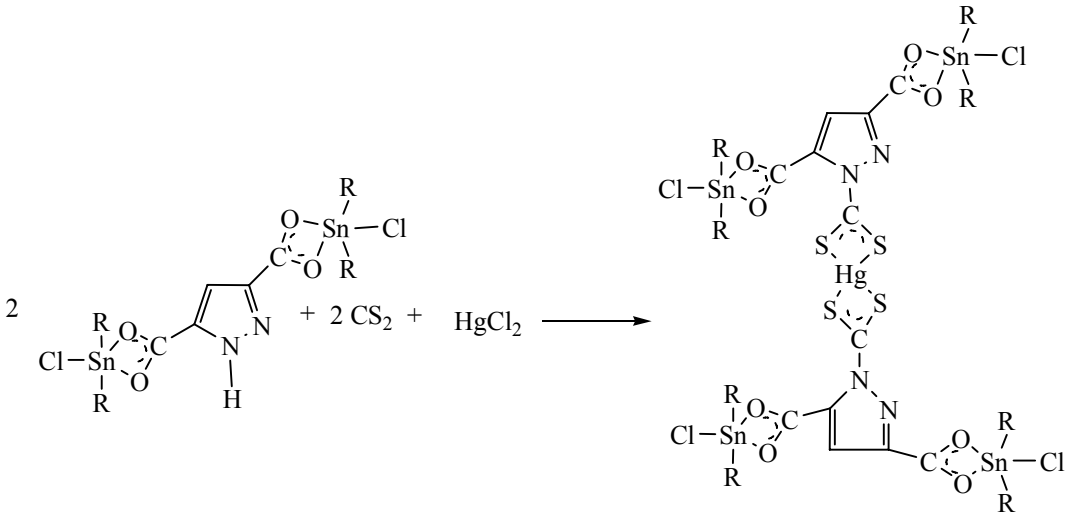

R = Me (**IV**), *n*-Bu (**V**), Ph (**VI**).

PM6 [12], PM3 [13, 14], AM1 [13], and MNDO [15] methods. Absence of imaginary frequencies was checked to confirm the global minimum in each case. The model was built by using constraints on the movement of each of four coordinated sulfur atoms and on Hg^{+2} ion on the *x,y,z* axes performing the geometry optimization. The geometry optimization was done without any constraints on any of the atoms. The final RMS values were always less than one. DFT calculations were performed in gas phase using Firefly QC package [16] which is partially based on the GAMESS (US) [16] source code using the BLYP exchange-correlation functional [17, 18], B3LYP hybrid functional [19, 20], *ab initio* calculations at the Hatree-Fock level of theory were carried out with the 3-21G basis set with Firefly QC pakage [21, 22].

Synthesis of compounds I–III. Pyrazole-3,5-dicaroxylic acid (1 mmol) was dissolved in methanol (20 mL) in a round bottom two necks flask with continuous stirring. Solid R_2SnCl_2 (R = Me, *n*-Bu, Ph) (2 mmol) was added in the above solution in portions. The reaction mixture was refluxed for 4 h. The solvent was evaporated slowly at room temperature. The product obtained was dried in the air and recrystallized from acetone : *n*-hexane (1 : 1) (Scheme 1).

Synthesis of compounds IV–VI. A solid product **I–III** (2 mmol) was dissolved in methanol (20 mL) in a 250 mL round bottom flask. CS_2 (2 mmol) was added drop wise in the above solution. The mixture was stirred for 0.5 h and solid $HgCl_2$ (1 mmol) was added in portions. The reaction mixture was stirred for 4 h at room temperature. The solvent was evaporated slowly at room temperature. A product obtained was dried in the air and recrystallized from methanol : *n*-hexane (1 : 1) (Scheme 2).

Synthesis of compounds VII and VIII. Pyrazole-3,5-dicaroxylic acid (1 mmol) was dissolved in methanol (20 mL) in a round bottom two necks flask

Scheme 3.

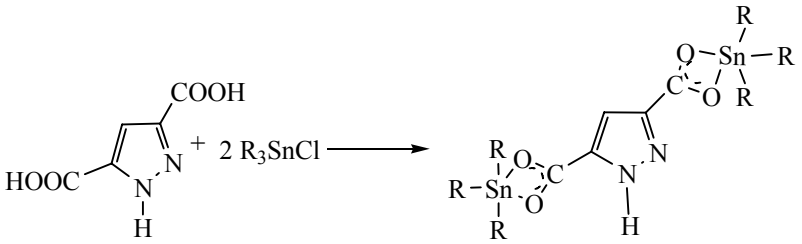

R = *n*-Bu (**VII**), Ph (**VIII**).

Scheme 4.

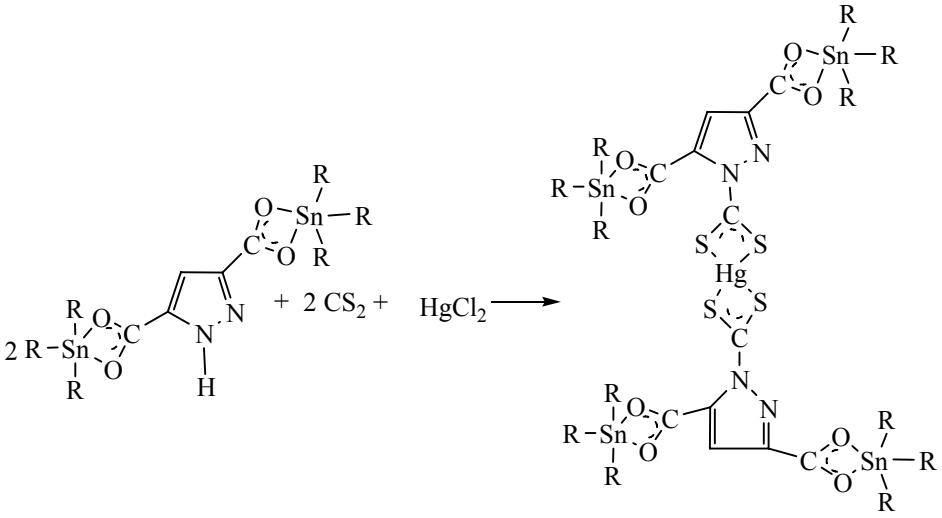

R = *n*-Bu (**IX**), Ph (**X**).

upon stirring. Solid R_3SnCl (R = *n*-Bu, Ph) (2 mmol) was added in the above solution in portions. The reaction mixture was refluxed for 6 h, the solvent was evaporated slowly at room temperature. The product obtained was dried in the air and recrystallized from acetone : *n*-hexane (1 : 1) (Scheme 3).

Synthesis of compounds IX and X. The solid product **VII** or **VIII** (2 mmol) was dissolved in methanol (20 mL) in a round bottom flask. Then CS_2 (2 mmol) was added drop wise in above solution and stirred for 30 min. Solid $HgCl_2$ (1 mmol) was added in portions and stirred for 6 h. The solvent was evaporated slowly at room temperature. The product was dried in the air and recrystallized from methanol : *n*-hexane (1 : 1) (Scheme 4).

RESULTS AND DISCUSSION

Physical data of products are listed in Table 1.

FT-IR spectra were recorded in the range of 4000–250 cm^{-1} as KBr/CsBr discs. The strong band at 3218 cm^{-1} characteristic for the NH group of the ligand was not recorded in the spectra of complexes **IV–VI**, **IX**, and **X**. In complexes **I–X** ν_{as}(COO) were observed in the range of 1642–1600 cm^{-1} and ν_s(COO) in the range of 1458–1425 cm^{-1}. It was noted that the value $\Delta\nu = \nu_{as}(COO) - \nu_s(COO)$ lower than 200 cm^{-1} indicated the bidentate carboxylate and higher than 200 cm^{-1} was typical for the monodentate carboxylate [23, 24]. Complexation of tin(IV) with the ligand was supported by the presence of Sn–O bands in the range 495–445 cm^{-1} [25] (Table 2).

It has been reported [26] that a single ν(C–S) band in the region around 1000 cm^{-1} was indicative of dithiocarbamate groups that were bonded symmetrically or bidentate in nature. Splitting of the band around 1000 cm^{-1} has been reported for dithiocarbamate groups that acted as a monodentate ligand or were

Table 1. Physical data of the synthesized complexes with pyrazole-3,5-dicarboxylic acid

Comp. no.	Molecular formula	Molecular weight, g/mol	Yield, %	mp, °C	Elemental analysis, %			
					C calculated (found)	H calculated (found)	N calculated (found)	S calculated (found)
HL	$C_5H_5O_5N_2$	174.11	–	290.0	–	–	–	–
I	$C_9H_{14}O_4Cl_2N_2Sn_2$	522.60	75	230.1	20.68 (20.64)	2.70 (2.75)	5.35 (5.31)	–
II	$C_{21}H_{38}O_4Cl_4N_2Sn_2$	690.914	77	235.6	36.50 (36.54)	5,54 (5.59)	4.05 (4.09)	–
III	$C_{29}H_{22}O_4Cl_4N_2Sn_2$	770.86	66	228.9	45.18 (45.13)	2.87 (2.81)	3.63 (3.67)	–
IV	$C_{20}H_{26}O_8S_4Sn_4HgN_4Cl_4$	1396.70	67	213.4	17.18 (17.21)	1.87 (1.91)	4.00 (4.04)	9.16 (9.12)
V	$C_{44}H_{74}O_8S_4Sn_4HgN_4Cl_4$	1733.09	95	240.1	30.46 (30.42)	4.30 (4.33)	3.23 (3.27)	7.38 (7.41)
VI	$C_{60}H_{42}O_8S_4Sn_4HgN_4Cl_4$	1892.83	65	255.6	38.03 (38.01)	2.23 (2.20)	2.95 (2.98)	6.76 (6.72)
VII	$C_{29}H_{56}O_4Cl_2N_2Sn_2$	734.13	73	268.9	47.44 (44.42)	7.68 (7.73))	3.81 (3.86)	–
VIII	$C_{41}H_{32}O_4Cl_2N_2Sn_2$	854.83	63	237.8	57.60 (57.65)	3.77 (3.81)	3.27 (3.22)	–
IX	$C_{60}H_{110}O_8S_4Sn_4HgN_4$	1819.38	65	120.1	39.57 (39.53)	6.09 (6.13)	3.07 (3.03)	7.03 (7.00)
X	$C_{84}H_{62}O_8S_4Sn_4HgN_4$	2058.99	70	185.6	48.95 (48.92)	3.03 (3.06)	2.71 (2.74)	6.21 (6.25)

asymmetrically bonded [27–29]. The compounds exhibited single ν(C–S) bands between 940 and 956 cm^{-1} which was attributed to bonding of two sulfur atoms with tin atom. Complexation of Sn(IV) and Hg(II) with the ligand was confirmed by the new bands recorded at 335–331 cm^{-1}, ν(Sn–Cl), and 287–279 cm^{-1}, ν(Hg–S) [30, 31].

^{1}H NMR spectra. ^{1}H NMR data of the ligand and complexes were recorded in DMSO-d_6. The number of protons observed in the spectra were in close agreement to those theoretically calculated by the incremental method [32]. The OH group signals (13.68 and 13.61 ppm) of the free ligand were not recorded in the spectra of complexes confirming deprotonation of the carboxylic group and its complexation with tin. The complexation did not cause significant change in the chemical shift for aromatic protons of the pyrazole ring. The values $^2J[^{119}Sn, ^1H]$ (82 and 81 Hz, respectively) for **III**, **VI**, **VIII,** and **X** supported the five coordinated environment around tin atom in solutions [33].

Compound I. Sn–CH_3Cl, 1.22 s, ^2J 97. **Compound II.** Sn–$CH_2CH_2CH_2CH_3Cl$, 0.86–0.94 m, 0.21 t (7.3). **Compound III.** Sn–C_6H_5Cl, 7.90 d, ^2J 82, 7.51–7.56 m, 7.41–7.49 m. **Compound IV.** Sn–CH_3Cl, 1.25 s, ^2J 95. **Compound V.** Sn–$CH_2CH_2CH_2CH_3Cl$, 0.85–0.95 m, 0.25 t (7.2). **Compound VI.** Sn–C_6H_5Cl, 7.94 d, ^2J 82, 7.52–7.58 m, 7.44–7.53 m. **Compound VII.** Sn–$CH_2CH_2CH_2CH_3$, 0.61–1.4 m, 0.25 t (7.2). **Compound VIII.** Sn–C_6H_5, 7.98 d ^2J 82, 7.56–7.61 m, 7.40–7.57 m. **Compound IX.** Sn–$CH_2CH_2CH_2CH_3$, 0.66–1.17 m, 0.28 t (7.2). **Compound X.** Sn–C_6H_5, 7.89 d, ^2J 81, 7.54–7.60 m, 7.42–7.59 m.

Table 2. IR data (cm^{-1}) of synthesized compounds with pyrazole-3,5-dicarboxylic acid

Comp. no.	ν(NH)	ν(COO)		Δν	ν(C=S)	ν(C–S)	ν(Sn–O)	ν(Sn–C)	ν(Hg–S)	ν(Sn–Cl)
		ν_{as}(COO)	ν_{s}(COO)							
HL	3218	1702	1491	211	–	–	–	–	–	–
I	3222	1642	1456	186	–	–	495	580	–	331
II	3228	1630	1425	195	–	–	453	560	–	334
III	3225	1615	1428	187	–	–	450	258	–	331
IV	–	1605	1442	163	1014	956	452	570	286	331
V	–	1610	1445	165	1015	985	455	590	287	335
VI	–	1685	1429	156	1015	985	452	250	279	332
VII	3221	1640	1458	182	–	–	448	580	–	–
VIII	3224	1605	1427	178	–	–	470	260	–	–
IX	–	1600	1458	142	1020	980	490	570	287	–
X	–	1628	1435	193	1010	985	445	252	285	–

^{13}C NMR spectra. Proton decoupled ^{13}C NMR spectra were recorded in DMSO-d_6. The data verified complexation of the ligand with tin and mercury. The spectra enabled to assign the number of non-equivalent carbon atoms and to identify the types of carbon atoms (butyl, aromatic, carbonyl etc.) [34]. The chemical shift at 161.8 ppm was assigned to carboxylate carbon (C^1 and $C^{1'}$) of the free ligand. This signal was shifted downfield (172.1–173.3 ppm) in the spectra of complexes **I–X**. The signal in the range 202.7–206.1 ppm in the spectra of complexes **IV–VI**, **IX,** and **X** provided the evidence for the CSS^- group coordination with mercury. The Hg–S linkage was evident from the S→Hg vibrational peak of the corresponding IR spectra of the complexes.

The carbon of phenyl and alkyl groups attached to tin were observed at almost similar positions as calculated from incremental method [32].

Compound I. Sn–CH_3Cl, (C^α) 28.1, ^1J 298. **Compound II.** Sn–C_4H_9Cl; (C^α) 28.3, ^1J 551, (C^β) 27.4 ^2J 24, (C^γ) 26.6, ^3J 65, (C^δ) 14.3. **Compound III.** Sn–C_6H_5Cl, (C^α) 147.5, ^1J 434, (C^b) 137.5, ^2J 34, (C^γ), 135.2, ^3J 43, (C^δ) 129.4. **Compound IV.** Sn–CH_3Cl, (C^α) 28.3, ^1J 299. **Compound V.** Sn–C_4H_9Cl; (C^α) 28.7, ^1J 551, (C^β) 27.2, ^2J 24, (C^γ) 26.5, ^3J 65, (C^δ) 14.1. **Compound VI.** Sn–C_6H_5Cl, (C^α) 147.3, ^1J 434, (C^β) 137.6, ^2J 34, (C^γ), 135.5 ^3J 43, (C^δ) 129.3. **Compound VII.** Sn–C_4H_9, (C^α) 28.6, ^1J 573, (C^β) 26.4, ^2J 23, (C^γ) 25.7, ^3J 65, (C^δ) 14.7. **Compound VIII.** Sn–C_6H_5, (C^α) 142.3, ^1J 638, (C^β) 136.2, ^2J 47.8, (C^γ) 135.3, ^3J 58, (C^δ) 129.4. **Compound IX.** Sn–C_4H_9, (C^α) 28.6, ^1J 573, (C^β) 26.3, ^2J 23, (C^γ) 25.4, ^3J 65, (C^δ) 14.2. **Compound X.** Sn–C_6H_5, (C^α), 142.1, ^1J 638, (C^β) 136.0, ^2J 47.8, (C^γ) 135.9, ^3J 58, (C^δ) 129.2.

Semi-empirical study. The calculated bond lengths and bond angles are all typical to organotin(IV) compounds [35]. The Hg ion lied on the plane formed by the four sulphur atoms: 0.00 Å (**IV**), 0.01 Å away (**V**), and 0.04 Å away (**X**). The Hg^{+2}–S bonds length of 2.73 Å have been observed in the dithiocarbamate complexes of Hg^{+2}. The PM6 method overestimated the longer Sn–O bond length, though other bonds including the shorter Sn–O bond, Sn–Cl and Sn–C were correctly estimated. The values were shorter than sum of van der Waals radii for these ions, 3.68 Å. The calculated dipole moments were, D: 0.001 (**IV**), 0.317 (**V**), 1.370 (**VI**). Substitution of chlorine with the phenyl group in the complex **X** reduced the electron density at Sn and increased the positive charge. The charge at the central Hg ion was however not affected.

DFT study. In the structure obtained for complex **I** by B3LYP-3-21G method the angle between the planes between two carboxylate groups (Sn^{10}–O^9–C^8–O^{20}) and (Sn^1–O^2–C^3–O^4) was 0.0° with two chloride groups diagonally opposite to each other. Similar structures were also obtained with by BLYP/3-21G

Table 3. Selected bond angles of complex **I**

Bond angle, deg	Method						
	DFT		*ab initio*	semi-empirical			
	BLYP/3-21G	B3LYP/3-21G	HF/3-21G	PM3	PM6	AM1	MNDO
O–Sn–O	O^2–Sn^1–O^4						
	57.8	57.2	52.0	51.9	48.7	55.5	40.7
	O^9–Sn^{10}–O^{20}						
	58.5	58.1	54.4	52.2	49.9	55.7	41.1
	O^4–C^3–O^2						
O–C–O	119.2	118.8	119.6	110.2	119.0	111.3	119.2
	O^9–C^8–O^{20}						
	118.5	117.8	117.7	109.5	117.6	110.8	118.7
C–Sn–Cl	C^{29}–Sn^1–Cl^{33}						
	103.6	103.8	105.7	106.1	109.8	104.9	123.1
	C^{25}–Sn^1–Cl^{33}						
	103.6	103.8	105.7	106.1	109.8	104.9	108.3
	C^{12}–Sn^{10}–Cl^{11}						
	103.0	103.8	104.3	105.4	108.8	104.2	107.9
	C^{16}–Sn^{10}–Cl^{11}						
	103.0	102.9	104.2	105.4	108.8	104.2	107.9
C–Sn–C	C^{12}–Sn^{10}–C^{16}						
	127.2	127.6	125.9	119.4	122.2	122.4	122.6
	C^{29}–Sn^1–C^{25}						
	127.9	128.0	125.3	119.9	122.43	122.8	123.1

Table 4. Selected bond lengths of complex **I**

Bond	Bond length, Å	Method						
		DFT		*ab initio*	semi-empirical			
		BLYP/3-21G	B3LYP/3-21G	HF/3-21G	PM3	PM6	AM1	MNDO
O–Sn (short)	Sn^1–O^2	2.13	2.09	2.01	2.02	2.12	2.24	2.00
	Sn^{10}–O^{20}	2.13	2.10	2.02	2.02	2.12	2.24	2.00
O–Sn (long)	Sn^1–O^4	2.52	2.52	2.77	2.62	2.93	2.33	3.31
	Sn^{10}–O^9	2.47	2.45	2.62	2.59	2.84	2.31	3.28
O–C (short)	C^3–O^4	1.28	1.26	1.22	1.24	1.23	1.28	1.24
	C^8–O^9	1.28	1.26	1.23	1.24	1.23	1.29	1.24
O–C (long)	C^8–O^{20}	1.36	1.34	1.33	1.32	1.33	1.30	1.33
	C^3–O^2	1.36	1.34	1.33	1.32	1.33	1.30	1.33
Sn–Cl	Sn^1–Cl^{33}	2.48	2.46	2.43	2.36	2.34	2.42	2.31
	Sn^{10}–Cl^{11}	2.49	2.46	2.44	2.36	2.35	2.42	2.31
Sn–C	Sn^1–C^{25}	2.17	2.15	2.14	2.09	2.11	2.08	2.08
	Sn^1–C^{29}	2.17	2.15	2.14	2.09	2.11	2.08	2.08
	Sn^{10}–C^{12}	2.17	2.15	2.14	2.09	2.11	2.08	2.08
	Sn^{10}–C^{16}	2.17	2.15	2.14	2.09	2.11	2.08	2.08

Table 5. Selected bond angles of complex **III**

Bond angle, deg	Method					
	DFT		*ab initio*	semi-empirical		
	BLYP/3-21G	B3LYP/3-21G	HF/3-21G	PM3	PM6	AM1
			O^2–Sn^1–O^4			
O–Sn–O	57.8	57.2	52.0	51.9	48.7	55.5
			O^9–Sn^{10}–O^{34}			
	59.1	58.8	57.5	52.0	49.5	55.7
			O^4–C^3–O^2			
	118.8	118.1	116.8	110.1	119.4	111.2
O–C–O			O^9–C^8–O^{34}			
	118.0	117.3	115.7	109.4	118.0	110.7
			C^{50}–Sn^1–Cl^{61}			
	101.8	101.7	102.2	104.9	108.7	104.3
			C^{39}–Sn^1–Cl^{61}			
C–Sn–Cl	101.8	101.7	102.2	104.9	108.7	104.3
			C^{12}–Sn^{10}–Cl^{11}			
	101.2	101.2	101.6	106.4	107.8	103.7
			C^{23}–Sn^{10}–Cl^{11}			
	101.2	101.2	101.6	106.4	107.8	103.7
			C^{12}–Sn^{10}–C^{23}			
	128.7	129.0	127.8	117.0	123.0	120.7
C–Sn–C			C^{39}–Sn^1–C^{50}			
	129.3	129.6	128.0	120.2	123.6	121.4

and semi-empirical PM3, PM6, MNDO, *ab initio* and AM1 methods.

The carboxylate oxygen (with the short C–O bond) was bound to tin with a longer Sn–O bond while the carboxylate oxygen (with the long C–O bond) was bound to tin with shorter Sn–O bond (Tables 3, 4). MNDO and PM6 methods probably overestimated the longer Sn–O bond length, though other bonds including Sn–Cl and Sn–C were correctly estimated. In bond angle estimations the MNDO and PM6 methods calculated a comparatively low value of O–Sn–O angle, while AM1 method computed a lower value of O–C–O angle. The dipole moment calculated by MNDO and PM6 methods was different from the rest DFT, *ab initio* and Semi-empirical methods.

Computed dipole moments of the complex **I**, D: 0.974 (BLYP/3-21G), 1.098142 (B3LYP/3-21G), 1.538965 (HF/3-21G), 1.262 (PM3), 2.074 (PM6), 1.048 (AM1), 2.020 (MNDO).

In the structure **III** obtained by B3LYP-3-21G method the planes between two carboxylate groups (Sn^{10}–O^9–C^8–O^{34}) and (Sn^1–O^2–C^3–O^4) were 0.0° with the two chloride groups diagonally opposite to each other. Similar structures were obtained with by BLYP/3-21G and semi-empirical PM3, PM6 and AM1 methods. (The MNDO method yielded a distorted structure, therefore is not considered.)

The carboxylate oxygen (with the short C–O bond) is bound to tin with a longer Sn–O bond while the carboxylate oxygen (with the long C–O bond) is bound to tin with shorter Sn–O bond (Tables 5, 6). The PM6 method probably overestimated the longer Sn–O bond length, though other bonds including Sn–Cl and Sn–C were correctly estimated. In bond angle estimations again the PM6 method calculated a comparatively low value of O–Sn–O angle, while AM1 method computed a lower value of O–C–O angle.

Computed dipole moments of the complex **III**, D: 1.093779 (BLYP/3-21G), 1.090595 (B3LYP/3-21G), 0.993010 (HF/3-21G), 1.004 (PM3), 2.046 (PM6), 1.236 (AM1).

Table 6. Selected bond lengths of complex **III**

Bond	Bond length, Å	Method					
		DFT		*ab initio*	semi-empirical		
		BLYP/3-21G	B3LYP/3-21G	HF/3-21G	PM3	PM6	AM1
O–Sn (short)	Sn^1–O^2	2.15	2.12	2.06	2.01	2.12	2.24
	Sn^{10}–O^{34}	2.15	2.12	2.06	2.01	2.12	2.24
O–Sn (long)	Sn^1–O^4	2.46	2.44	2.46	2.63	2.94	2.33
	Sn^{10}–O^9	2.41	2.38	2.40	2.60	2.87	2.31
O–C (short)	C^3–O^4	1.29	1.27	1.24	1.24	1.23	1.28
	C^8–O^9	1.29	1.27	1.25	1.24	1.23	1.29
O–C (long)	C^8–O^{34}	1.34	1.33	1.31	1.32	1.33	1.30
	C^3–O^2	1.35	1.33	1.31	1.32	1.33	1.30
Sn–Cl	Sn^1–Cl^{61}	2.48	2.46	2.45	2.36	2.34	2.42
	Sn^{10}–Cl^{11}	2.49	2.47	2.46	2.36	2.35	2.43
Sn–C	Sn^1–C^{39}	2.15	2.13	2.12	2.04	2.10	2.08
	Sn^1–C^{50}	2.15	2.13	2.12	2.04	2.10	2.08
	Sn^{10}–C^{12}	2.15	2.13	2.12	2.04	2.10	2.09
	Sn^{10}–C^{23}	2.15	2.13	1.12	2.04	2.10	2.09

CONCLUSIONS

IR data confirmed trigonal bipyramid and square planar geometry around Sn(IV) and Hg(II), respectively. The bonding behavior was verified by semi-empirical study. NMR data revealed the 4-coordinated geometry of products in solutions. Charge calculations by semi-empirical method indicated that substitution of chlorine with aryl groups increased the positive charge in complex **X** as compared to complex **IV** and **V** due to decrease of electron density at Sn(IV) while the charge at the central Hg ion was not affected. The PM6 method calculated comparatively low value of O–Sn–O angle, while AM1 method computed a lower value of O–C–O angle for complex **I** and **III**.

ACKNOWLEDGMENTS

SKS and KQ thanks the Head, App Sci. and Dean FET, MITS for encouragement and support.

REFERENCES

1. Singh, H.L. and Varshney, A.K., *Appl. Organomet. Chem.,* 2001, vol. 15, p. 762.
2. Nath, M., Sulaxna, X., Song, X., and Eng, G., *J. Organomet. Chem.,* 2006, vol. 691, p. 1649.
3. Gielehn, M. and Tiekink, E., *Metallotherapeutic Drugs and Metal-Based Diagnostic Agents: The Use of Metals in Medicine*, Wiley, 2005.
4. Gielehn, M., *Tin Chemistry: Fundamentals, Frontiers, and Applications*, Alwyn, M.G., Davies, G., Pannell, K., and Tiekink, E., Eds., Wiley, 2008.
5. Molloy, K.C., Purcell, T.G., Hahn, E., Schumann, H., and Zukerman, J.J., *Organometallics,* 1986, vol. 5, p. 79.
6. Holmes, R.R., *Acc. Chem. Res.,* 1989, vol. 22, p. 190.
7. Barbieri, R., Silvestri, A., Lo Giudice, M., Ruisi, G., and Musmeci, M.T., *J. Chem. Soc., Dalton Trans.,* 1989, p. 519.
8. Sadiq-ur-Rehman, Shahid, K., Ali, S., Bhatti, M.H., and Parvez, M., *J. Organomet. Chem.,* 2005, vol. 690, p. 1396.
9. Rafiq, M., Ali, S., Shahzadi, S., Shahid, M., Sharma, S.K., and Qanungo, K., *J. Iran. Chem. Soc.,* 2014, vol. 11, p. 169.
10. Armarego, W.L.F. and Chai, C.L.L., *Purification of Laboratory Chemicals*, New York: Elsevier, 2003.
11. *MOPAC2007*, Stewart, J.J.P., Stewart Computational, Chemistry, Version: 7.334W.
12. Stewart, J.J.P., *J. Mol. Mod.,* 2007, vol. 13, p. 1173.
13. Stewart, J.J.P., *J. Mol. Mod.,* 2004, vol. 10, p. 155.

14. Dewar, M.J.S., Zoebisch, E.G., Healy, E.F., and Stewart, J.J.P., *J. Am. Chem. Soc.,* 1985, vol. 107, p. 3902.
15. Dewar, M.J.S., Thiel, W., *J. Am. Chem. Soc.,* 1977, vol. 99, p. 4899.
16. Granovsky, A.A., *Firefly version 7.1.G*, http://classic.chem.msu.su/gran/firefly/index.html.
17. Schmidt, M.W., Baldridge, K.K., Boatz, J.A., Elbert, S.T., Gordon, M.S., Jensen, J.H., Koseki, S., Matsunaga, N., Nguyen, K.A., Su, S., Windus, T.L., Dupuis, M., and Montgomery, J.A., *J. Comput. Chem.,* 1993, vol. 14, p. 1347.
18. Becke, A.D., *Phys. Rev. A.,* 1988, vol. 38, p. 3098.
19. Lee, C., Yang, W., and Parr, R.G., *Phys. Rev. B.,* 1988, vol. 37, p. 785.
20. Stephens, P.J., Devlin, F., Chabalowski, C.F., and Frisch, M.J., *J. Phys. Chem.,* 1994, vol. 98, p. 11623.
21. Binkley, J.S., Pople, J.A., Hehre, W.J., *J. Am. Chem. Soc.,* 1980, vol. 102, p. 939.
22. Gordon, M.S., Binkley, J.S., Pople, J.A., Pietro, W.J., and Hehre, W.J., *J. Am. Chem. Soc.,* 1982, vol. 104, p. 2797.
23. Xie, Q., Yang, Z., and Jiang, L., *Main Group Met. Chem.,* 1996, vol. 19, p. 509.
24. Xueqing, S., Zhiqiang, Y., Qinglan, X., and Jinshan, L., *J. Organomet. Chem.,* 1998, vol. 566, p. 103.
25. Ali, S., Khokhar, M.N., Bhatti, M.H., Mazhar, M., Masood, M.T., Shahid, K., and Badshah, A., *Synth. React. Inorg. Met.-Org. Chem.,* 2002, vol. 32, p. 1373.
26. Nath, M., Pokharia, S., Eng, G., Song, X., and Kumar, A., *J. Organomet. Chem.,* 2003, vol. 669, p. 109.
27. Amin, M.M., Ali, S., Shahzadi, S., Sharma, S.K., and Qanungo, K., *J. Coord. Chem.,* 2011, vol. 64, p. 337.
28. Nath, M., Jairath, R., Eng, G., Song, X., and Kumar, A., *Spectrochim. Acta, Part A.,* 2005, vol. 62, p. 1179.
29. Kumar, A. and Garg, W., *Inorg. Chim. Acta,* 2006, vol. 346, p. 227.
30. Singh, R. and Kaushik, N.K., *Spectrochim. Acta, Part A.,* 2008, vol. 71, p. 669.
31. Khoo, E., Goh, N.K., Eng, G., Whalen, D.J., and Hzell, A., *Appl. Organomet. Chem.,* 1995, vol. 9, p. 699.
32. Kalinowski, H.O., Berger, S., and Brown, S., *^{13}C NMR Spectroskopie*, Stuttgart: Thieme, 1984.
33. Molloy, K.C., in *The Chemistry of Metal-Carbon Bond*; Hartly, F., Ed.; New York: Wiley, 1989.
34. Holecek, J., Nadvornik, M., Handlir, K., and Lyacka, A., *J. Organomet. Chem.,* 1986, vol. 315, p. 299.
35. Shahzadi, S. and Ali, S., *J. Iran. Chem. Soc.,* 2008, vol. 5, p. 16.